Theoretical Metastability of Semiconductor Crystallites in High-Pressure Phases, with Application to β-Tin Structure Silicon

L. E. Brus,* J. A. W. Harkless, and F. H. Stillinger

Contribution from AT&T Bell Laboratories, Murray Hill, New Jersey 07974-0636

Received December 11, 1995[⊗]

Abstract: We examine prospects for metastability of six-coordinate high-pressure semiconductor phases at ambient temperature and pressure (STP). We investigate a simple "thermodynamic", coherent transformation model for nanocrystals of size >2 nm and, as a quantitative example, apply it to the silicon β-tin to diamond structural phase transition. The unit cell transformation path is taken from a calculation by Mizushima et al. (Mizushima, K.; Yip, S.; Kaxiras, E. *Phys. Rev.* **1994**, *B50*, 14952). Surface energies and the initial crystallite shape are included in an absolute rate model. The model assumes that the crystallite shape substantially changes to accommodate the unit cell *c*/*a* variation from 1.414 (diamond) to 0.55 (β-tin). The model predicts that the β-tin nanocrystal lifetime increases rapidly with increasing size. Near-round β-tin nanocrystals are more stable and have slower transformation rates than oblate spheroid nanocrystals with larger surface energy. For size >2 nm, both near-round and oblate β-tin nanocrystals are metastable with half-lives of years or more. An alternate, classical nucleation model is considered for surface nucleation in larger microcrystals. In this model the β-tin nanocrystal lifetime decreases with increasing size. Yet micron-size and smaller crystallites are metastable as well. Defect and strain-free β-tin microcrystals appear to be metastable at STP. More generally, stabilization of high-pressure semiconductor phases at STP should be more widespread in nanocrystals than in bulk crystals, because of (1) the relative ease in annealing out defects, strain, and impurities in nanocrystals and (2) the use of surface passivation in lowering the surface energy of the high-pressure phase.

1. Introduction

Tetrahedrally bonded semiconductors have a rich structure of high-pressure and -temperature solid phases, in which density and atomic coordination generally increase. Substantial hysteresis is often observed in their solid−solid phase transitions, which implies that large kinetic barriers are present for such first-order transitions with substantial volume changes. Several examples are known of high-pressure phases that are indefinitely metastable at STP. Four-coordinate, thermodynamically stable, wurtzite AlN is a 6.2 eV band gap, III−V semiconductor. Six-coordinate rock salt AlN, with a ∼2.0 eV band gap, can be made by pressurization of wurtzite AlN and is metastable at STP upon pressure release.[1a−c] Macroscopic amounts have been made in a high-temperature and -pressure anvil apparatus.[1a] Wurtzite MgTe, synthesized at high temperature and stable indefinitely at STP, is now thought to be metastable with respect to the NiAs structure phase, for which in fact no facile synthesis is known.[1d] In a related example, ∼100 μm single crystals of stishovite SiO_2, in which Si is six-coordinate, have been recovered from high-temperature and -pressure anvil synthesis.[1e,f] Stishovite is thermodynamically stable only above 8.1 GPa at 23 °C. In thermodynamically stable α-quartz at STP, Si is four-coordinate. Stishovite has a 60% smaller volume and a 30% larger optical refractive index than quartz.

Faceted nanocrystals of metastable, indirect gap rock salt CdS have been made by using surfactants to control precipitation in a thin polyethylene oxide film at STP.[2] Normally CdS is found only in the direct gap, tetrahedrally bonded wurtzite and zinc blende phase; rock salt is a high-pressure phase, as in the AlN system. The mechanism is not well understood.

The transformation kinetics between solid phases in semiconductors are not understood. They are different experimentally in nanocrystals compared to bulk crystals. Quite generally, in nanocrystals the thermodynamic phase diagram in the temperature−pressure plane, and the kinetics, should become size dependent as surface energies become significant. Recent studies by Tolbert, Alivisatos, and co-workers, on CdSe and Si nanocrystals, show size-dependent changes in both the thermodynamics and kinetics as a function of pressure.[3] In the size ranges investigated, just one "nucleation" event per nanocrystal is observed. A single crystallite of one phase transforms into a single crystallite of another phase. As a consequence, the shape of the nanocrystal changes to reflect the distortion of the unit cell upon phase transition, as experimentally observed in 50 nm Si nanocrystals.[3d,e]

Different results are obtained in kinetic studies of bulk samples. For example, in a careful study of the four-coordinate to six-coordinate transition in high-quality, ∼50 μm GaAs crystals, shape did not change.[4] Instead, multiple nucleation and fragmentation into 5−10 nm domains was observed. The various zinc blende GaAs physical properties did not change simultaneously with increasing pressure, as should occur in a

[⊗] Abstract published in *Advance ACS Abstracts,* May 1, 1996.

(1) (a) Vollstadt, H.; Ito, E.; Akaishi, M.; Akimoto, S.; Fukunaga, O. *Proc. Jpn. Acad. Ser.* **1990**, *B66*, 7. (b) Gorczyca, I.; Christensen, N.; Perlin, P.; Grzegory, I.; Jun, J.; Bockowki, M. *Solid State Commun.* **1991**, *79*, 1033. (c) Xia, Q.; Xia, H.; Ruoff, A. *J. Appl. Phys.* **1993**, *73*, 8198. (d) Li, T.; Luo, H.; Greene, R.; Ruoff, A.; Trail, S.; DiSalvo, F. *Phys. Rev. Lett.* **1995**, *74*, 5232. (e) Stishovite, S.; Popova, S. *Geochemistry (Engl. Transl.)* **1961**, *10*, 923. (f) Lin, L.; Bassett, W.; Takahaski, T. *J. Geophys. Res.* **1974**, *79*, 1161.

(2) Lin, J.; Cates, E.; Bianconi, P. *J. Am. Chem. Soc.* **1994**, *116*, 4738.

(3) (a) Tolbert, S.; Alivisatos, A. P. *Science* **1994**, *265*, 373 and references contained therein. (b) Tolbert, S.; Alivisatos, A. P. *J. Chem. Phys.* **1995**, *102*, 1. (c) Tolbert, S.; Herhold, A.; Johnson, C.; Alivisatos, A. P. *Phys. Rev. Lett.* **1994**, *73*, 3166. (d) Tolbert, S.; et al. Pressure Induced Structural Transformations in Si Nanocrystals: Surface and Shape Effects. Submitted to *Phys. Rev. Lett.* (e) Tolbert, S.; Alivisatos, A. P. *Annu. Rev. Phys. Chem.* **1995**, *46*, 595.

(4) Besson, J.; et al. *Phys. Rev.* **1991**, *B44*, 4214.

S0002-7863(95)04166-7 CCC: $12.00

first-order transition. Extended planar defects formed as the material slowly converted. These differences with the nanocrystal kinetics are suggested to be related to relief of volume-change-induced stress in the macroscopic crystal.

In the microelectronics industry such ideas may become important as device size decreases toward 0.05−0.1 μm. For example, bulk diamond lattice silicon under pressure undergoes a tetragonal distortion into a six-coordinate β-tin, metallic structure that is about 0.25 eV/atom higher in energy at 1 atm. Mizushima,Yip, and Kaxiras (hereafter MYK) have shown that, while the thermodynamic transformation can occur at about 8 GPa, the defect-free lattice remains kinetically stable, in both *ab initio* calculations and molecular dynamics simulations, up to 64 GPa.[5] In the defect-free bulk a huge kinetic barrier to conversion and reversion is predicted by these calculations. Thus β-tin silicon might be a metastable material of use in microelectronics.

The MYK calculation does not include possible size or surface effects. This report describes an attempt to understand the conditions under which bare β-tin silicon crystallites might be kinetically stable at STP. This silicon transition is prototypical of the six- to four-coordinate transitions observed in tetrahedral semiconductors. We develop a simple, coherent deformation, transition state theory of a type that might be used for isomerization in a large molecule, and we apply it to nanocrystals of diameter 2 nm and larger. Our model includes both bulk and surface free energies. In larger crystallites we consider a classical fluctuation phase transition mechanism.

2. Crystalline Phases of Silicon

The thermodynamically stable form of elemental silicon at STP displays the diamond lattice cubic structure.[6] Each atom in this allotrope bonds covalently to four other equivalent nearest neighbors in an undistorted tetrahedral pattern, with a bond length of 2.35 Å. The unit cell in this diamond cubic structure contains eight atoms. Intensive experimental and theoretical examinations of elemental silicon throughout the temperature−pressure plane have revealed the existence of a diverse collection of alternative crystalline phases. Upon raising the pressure to approximately 11 GPa, the diamond cubic form undergoes a first-order phase change to a tetragonal β-tin structure,[7] and as a result the initially semiconducting silicon becomes metallic. As shown in Figure 1, this phase change involves a substantial decrease in the crystallographic c/a ratio from 1.414 to 0.55 that flattens the tetrahedral neighbor grouping in the diamond cubic structure, while bringing two other atoms into close proximity to increase the coordination number from 4 to 6. The β-tin unit cell contains four atoms. Further increase in pressure induces a sequence of further phase transformations, the result of each of which presumably represents a region of thermodynamic stability in the temperature−pressure plane. At about 13 GPa, the β-tin form experiences a second-order transition to a body-centered orthorhombic *Imma* phase.[8] This is followed by another second-order transition, at 16 GPa, to a simple hexagonal (sh) form.[9] A hexagonal close packed (hcp) allotrope becomes stable at about 40 GPa.[10] Theoretical studies[11] suggest that the hcp form gives way to a face-centered cubic (fcc) form at approximately 120 GPa.

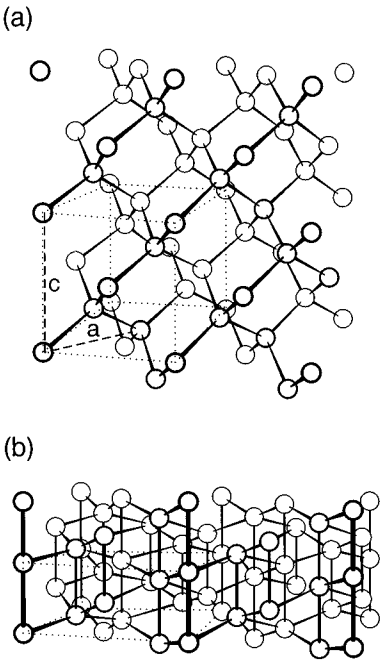

Figure 1. (a) Schematic drawing of diamond cubic Si. The unit cell is shown in dashed lines. (b) β-Tin Si also showing the unit cell.

In addition to these thermodynamically stable allotropes, several metastable solid phases formed under nonequilibrium conditions have also been reported. These include the distorted tetrahedral BC8 structure and solid amorphous silicon.[12,13]

3. Nanocrystal Energies

Parts a and b of Figure 1 illlustrate the bulk atomic bonding patterns that exist in the diamond cubic and β-tin allotropes. MYK have performed *ab initio* local density functional calculations to evaluate the electronic energy ΔE_b of the bulk material along the lowest energy, continuous deformation path between the two phases. Both the unit cell volume and c/a change along this transition pathway. Their zero-pressure results, on a per-atom basis and relative to the diamond cubic endpoint, can be fitted to the simple form (expressed in ergs/atom)

$$\Delta E_b/N = 10^{-13}\{X[2^{1/2} - (c/a)]^2 - Y[2^{1/2} - (c/a)]^4 + Z[2^{1/2} - (c/a)]^n\} \quad (3.1)$$

where N is the number of atoms and X, Y, Z, and n are fitting parameters:

$$X = 30.7167$$
$$Y = 42.7787$$
$$Z = 22.3784$$
$$n = 10.9523 \quad (3.2)$$

In order to include size and shape effects, we will model nanocrystal energies as a simple sum of an interior energy and a surface energy. Surface energies depend upon the type of facet exposed in both the stable diamond cubic phase and the β-tin phase and would be expected to vary with c/a along the deformation path. Eaglesham et al.[14] studied voids in diamond cubic Si and found that the mean surface energy is 1340 erg/

(5) Mizushima, K.; Yip, S.; Kaxiras, E. *Phys Rev.* **1994**, *B50*, 14952.
(6) Donohue, J. *The Structure of the Elements*; Krieger Publ. Co.: Malabas, FL, 1974; p 262.
(7) (a) Fameson, J. *Science* **1983**, *39*, 762. (b) Weinstein, B.; Piermarini, P. *Phys. Rev.* **1975**, *B12*, 1172.
(8) McMahon, M.; Nelmes, R. *Phys. Rev.* **1993**, *B47*, 8337.
(9) (a) Olijnyk, H.; Sikka, S.; Holtzapfel, W. *Phys. Lett.* **1984**, *103A*, 127. (b) Hu, J.; Spain, I. *Solid State Commun.* **1984**, *51*, 263.
(10) Zhu, H.; Merkle, L.; Menoni, C.; Spain, I. *Phys. Rev.* **1986**, *B34*, 4679.
(11) Chang, K.; Cohen, M. *Phys. Rev.* **1985**, *B31*, 7819.
(12) (a) Wentorf, R., Jr.; Kasper, J. *Science* **1963**, *129*, 338. (b) Bundy, F. *J. Chem. Phys.* **1964**, *41*, 3809.
(13) Imai, M.; Yaoita, K.; Katayama, K.; Chen, J.; Tsuji, K. *J. Non-Cryst. Solids* **1992**, *150*, 49.
(14) Eaglesham, D.; White, A.; Feldman, L.; Moriya, N.; Jacobson, D. *Phys. Rev. Lett.* **1993**, *70*, 1643.

cm^2. Within 10% the surface energy is the same for the reconstructed 001 and 111 facets at equilibrium. It is instructive to compare this experimental average surface energy for diamond cubic to an elementary estimate based upon the planar density of Si−Si covalent bonds that would be cut by a randomly inserted plane dividing the diamond cubic crystal into two parts. This estimate, 2202 erg/cm^2, depends upon the bulk diamond cubic heat of formation and lattice constant, but assumes no surface reconstruction. The discrepancy between this naive estimate and the experimental value measured by the ratio $R = 1340/2202 \approx 0.6085$ emphasizes the importance of surface reconstruction in lowering the energy of the crystal surface.

We are not aware of either experimental or theoretical values for the surface energies of β-tin Si, or for the distorted structures between the two phases. We roughly approximate these values by assuming (a) that isotropy continues to be a reasonable approximation as a function of c/a, (b) that for six-coordinate β-tin a cutting plane estimate renormalized by the surface reconstruction factor 0.6085 gives an adequate approximation to the surface energy, and (c) that a linear interpolation in c/a is valid to estimate the surface energies between the two end-point phases. Consequently we arrive at the simple expression for surface energy γ (in ergs/cm^2)

$$\gamma(c/a) = 2199.1 - 607.49(c/a) \qquad (3.3)$$

This, along with the bulk energy expression 3.1, will form the basis for our nanocrystal energy calculations. In equation 3.3 β-tin silicon has the higher surface energy.

4. Coherent Deformation Model

It is not known whether nanocrystals change phase by a simultaneous coherent deformation of all unit cells or deformation occurs locally and subsequently propagates across the nanocrystal. In both models the nanocrystal will change shape if there is just one nucleation event. In the small size limit where the nanocrystal size is equal to the bulk critical nucleus size, transformation should occur by fluctuation of the entire nanocrystal. We now consider such a coherent deformation model and apply simple absolute rate theory.

At 1 atm the volume per Si atom V decreases from 20.019×10^{-3} nm^3 in the diamond cubic form to 14.6×10^{-3} nm^3 in the β-tin form, as estimated from Figure 1 in ref 5. For present purposes we simply assume that along the reaction path the volume per Si atom is linear in c/a variation between the two end phases. This yields

$$V(c/a) = \{6.2704(c/a) + 11.1513\} \times 10^{-3}\ \text{nm}^3 \qquad (4.1)$$

Consider several shape-dependent transition pathways as shown in Figure 2. In process I a near-spherical diamond cubic nanocrystal coherently decreases in c/a to the β-tin value. The sphere deforms into an oblate spheroid with smaller volume as indicated by eq 4.1. Process I′ is simply the reverse transformation of the oblate spheroid, β-tin nanocrystal. These two processes correspond to a pressurization−depressurization cycle (referred to 1 atm pressure), without a possible shape change due to thermal annealing in the intermediate β-tin phase. If such annealing does occur, then in process II′ a near-spherical β-tin nanocrystal increases in c/a value to the diamond lattice value and distorts into a larger-volume prolate spheroid. Process II itself is the transformation of a prolate spheroid diamond lattice nanocrystal into a spherical β-tin nanocrystal. In these

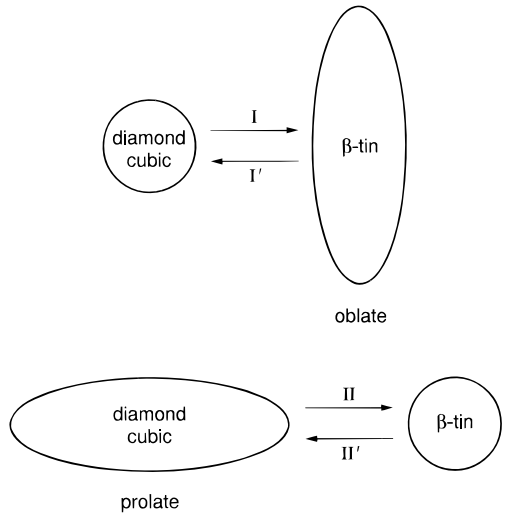

Figure 2. Shape-dependent transition pathways as described in the text.

processes, the energy of a nanocrystal as a function of shape and c/a ratio is

$$\Delta E(N,c/a) = \Delta E_b(c/a) + \gamma(c/a)\, S(N,c/a) \qquad (4.2)$$

where $S(N,c/a)$ is the nanocrystal surface area, and the other quantities have been previously defined.

Oblate and prolate spheroids are characterizated by major (A) and minor (B) axes. In our coherent deformation processes,

$$B = 2^{-1/2}Ac/a \qquad \text{(processes I, I′)} \qquad (4.3)$$

$$B = 0.55A(c/a)^{-1} \qquad \text{(processes II, II′)}$$

A and B define ϵ, the spheroid eccentricity parameter,

$$\epsilon = (A^2 - B^2)^{1/2}/A \qquad (4.4)$$

ϵ is implicitly a function of c/a. The expressions for nanocrystal volume and surface area are as follows:

processes I and I′

$$NV(c/a) = \pi A^2 B/6 \qquad (4.5)$$

$$S = \pi A^2/2 + (\pi B^2/4\epsilon)\ln[(1+\epsilon)/(1-\epsilon)] \qquad (4.6)$$

processes II and II′

$$NV(c/a) = \pi AB^2/6 \qquad (4.7)$$

$$S = \pi B^2/2 + (\pi AB/2\epsilon)\arcsin(\epsilon) \qquad (4.8)$$

Upon selection of values for N and c/a, eq 4.3 and eq 4.5 or 4.7 specify A and B. This allows ϵ and then S to be evaluated. Finally eq 4.2 yields the energy relative to bulk diamond cubic silicon.

The preceding formulas for numerical calculation of $\Delta E(N,c/a)$ constitute a relatively crude model of Si nanocrystal coherent deformation energetics. Yet we believe this model to provide a qualitatively useful guide for future experimental and theoretical work. Figure 3 exhibits ΔE vs c/a, calculated for $N = 100$. For processes I and I′, there is a well-defined β-tin local minimum in c/a at 0.584. This value is shifted from the bulk value of $c/a = 0.55$ by the effect of surface energy. The ΔE maximum at $c/a = 0.751$ provides a kinetic barrier $\Delta E^{\ddagger}$ for transformation of the β-tin nanocrystal into the lower energy diamond cubic nanocrystal.

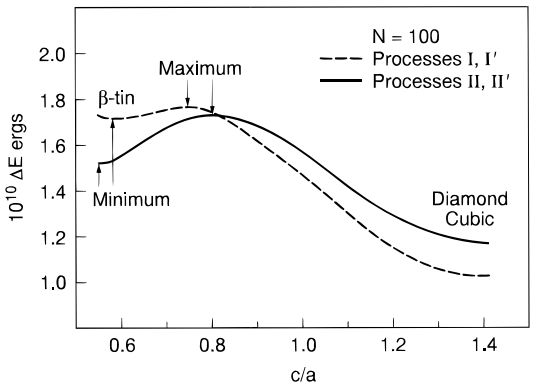

Figure 3. Transformation energy ΔE per nanocrystal versus c/a for $N = 100$. Note that 10^{-10} erg/nanocrystal is equivalent to 1440 kcal/mol of nanocrystals.

Table 1

	process I′		process II′	
N	$\Delta E^{\ddagger}$, erg	$t_{1/2}$ (300 K), s	$\Delta E^{\ddagger}$, erg	$t_{1/2}$ (300 K), s
50	1.0×10^{-11}	1.2×10^{97}	1.9×10^{-12}	7.0×10^{6}
60	1.3×10^{-11}	5.0×10^{118}	2.7×10^{-12}	1.5×10^{15}
70	1.5×10^{-11}	2.0×10^{140}	3.5×10^{-12}	1.4×10^{24}
80	1.7×10^{-11}	7.6×10^{161}	4.4×10^{-12}	4.4×10^{33}
90	1.0×10^{-11}	2.7×10^{183}	5.4×10^{-12}	3.9×10^{43}
100	2.0×10^{-11}	9.1×10^{204}	6.4×10^{-12}	7.9×10^{53}

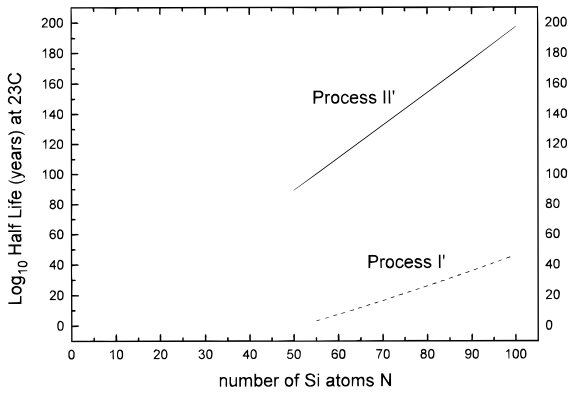

Figure 4. Logarithmic plot of β-tin nanocrystal half-life in years versus N.

For the II and II′ pathway, the β-tin local minimum is at the bulk value 0.55, since the spherical nanocrystal surface at the pathway end point is an extremal surface. The maximum now appears at $c/a = 0.806$ and defines a substantially higher energy barrier. Table 1 contains the activation barrier heights $\Delta E^{\ddagger}$ for a range of N. Figure 4 and Table 1 show β-tin half-lives $\tau_{1/2}$ at 300 K, based upon application of an elementary version of absolute rate theory:

$$\tau_{1/2}(T) = [(\ln 2)h/k_{\mathrm{B}}T] \exp[\Delta E^{\ddagger}/k_{\mathrm{B}}T] \qquad (4.9)$$

where h and k_{B} have their usual meanings. Expression 4.9 implicitly assumes that the vibrational free energy is substantially constant along the reaction pathway.

Within this model, there is a very large shape effect. In Figure 4, a round β-tin nanocrystal is far more stable than an oblate nanocrystal with higher surface area. Yet, even an oblate nanocrystal has a half-life of more than 1 year for $N > 50$ Si atoms, corresponding to ~2 nm size. For $N = 70$, process I has an activation barrier of 9.3 eV, and process II has an activation barrier of 2.2 eV. The barriers are high even for small size, because chemical bonds are quite strong and directional in silicon. Both processes I and II have increasing activation barriers as N increases. In the limit that surface energies are small with respect to bulk energies, the activation barrier scales as N^{3}. We have not extented the calculations below roughly $N = 50$, as the model is not applicable to reconstructed silicon clusters with few interior atoms.

5. Classical Nucleation Model

The coherent deformation model does not experimentally apply to large crystals, for example the ~50 μm GaAs crystals mentioned in the Introduction. In large β-tin crystallites, other mechanisms may dominate the very slow coherent process. In classical nucleation theory, a small spatial region of β-tin is postulated to fluctuate thermally into the diamond phase. There is an activation barrier because of the high-energy interface created between the four-coordinate diamond and six-coordinate β-tin phases. There is an additional strain barrier due to accommodation of the shape and volume change. At the critical nucleus size, the transformation propagates. In transitions with large volume changes, nucleation is thought to be more favorable on grain boundary surfaces than inside the bulk, in order to reduce the strain associated with volume change, and to lower the interface activation energy.[15] In crystallites, surface nucleation should be favored. This classical model might be correct in the limit that particle size is large with respect to the width of the two-phase interface. With just one nucleation event per particle, a particle shape change as we describe will occur. As each surface atom can serve as a nucleation center, the rate of nucleation K increases with increasing particle size.

Christian gives the following expression for the critical activation energy ΔG^{s} of a nucleus of phase "β" at the surface of a macroscopic phase "α" domain:[15]

$$\Delta G^{\mathrm{s}} = \frac{4\pi\sigma^{3}\upsilon^{2}(2 - 3\cos\theta + \cos^{3}\theta)}{3(g_{\beta} - g_{\alpha})^{2}}$$

$$K\,(\mathrm{s}^{-1}) = N_{\mathrm{s}}\left(\frac{kT}{h}\right)\exp\left(\frac{-\Delta G^{\mathrm{s}}}{kT}\right)$$

where $\cos\theta = (\gamma_{\alpha} - \gamma_{\beta})/\sigma$, σ is the interface energy between the two solid phases, γ is the surface energy of a single phase as defined earlier, υ is the atomic volume in the initial phase α, and $g_{\alpha} - g_{\beta}$ is the difference in free energies per atom. $K\,(\mathrm{s}^{-1})$ is the unimolecular rate of phase transformation per particle, where N_{s} is the number of surface atoms. K is proportional to the surface area. We neglect the additional strain energy.

We apply these formulas to nucleation of diamond Si at the surface of a large β-tin particle. The difference in free energies is 0.25 eV/atom from MYK. The surface energies and atomic volume have been stated previously. σ, the interface energy between four-coordinate diamond Si and six-coordinate β-tin Si, is uncertain. We take $\sigma = 1920$ erg/cm^{2}, which is the experimental value for σ between a six-coordinate high-pressure phase of AlAs and the four-coordinate zinc blende phase of GaAs, as reported in a high-pressure experiment on an AlAs:GaAs superlattice.[16] This value happens to be about the same as our rough estimate of the surface energy γ of the silicon β-tin phase itself.

With these parameters, $\Delta g^{\mathrm{s}} = 58$ eV, and the rate K is extraordinarily slow, even for macroscopic (cm size) β-tin particles. Interface energies in such strongly bonded materials are so high that classical fluctuation nucleation is negligible.

6. Discussion

A. Nucleation Mechanisms. How does nucleation occur? Solid−solid displacive phase transitions such as we model are

(15) Christian, J. W. *The Theory of Transformations in Metals and Alloys*, 2nd ed.; Pergamon: Oxford, 1975; Part 1, Section 52.

(16) Cui, L.; Venkateswaran, U.; Weinstein, B.; Chambers, F. *Phys. Rev.* **1992**, *B45*, 9248.

perhaps best understood in martensitic materials. Iron and ferrous alloys made at very high temperature undergo a cubic to tetragonal first-order phase transition upon cooling, near 850 °C. Strain energy from a shear-dominant lattice distortion controls the kinetics and final domain morphology. The unit cell distortion (here labeled Bain distortion) causes an initially spherical region to become elliptical, as in our Si nanocrystals. *In bulk samples, the transition is thought to be always extrinsically nucleated, typically by the strain fields of dislocations*.[17] Nucleation in nanocrystals and microcrystals of these materials has been studied in defect-free, yet coherently strained precipitates formed at high temperature in copper-rich alloys.[18] Nanocrystal hysteresis upon cooling is far larger than in bulk for the same driving force, and in some cases the fcc austenite particle is metastable at 23 °C, as an inclusion and even upon removal from the host. Externally applied strain can nucleate the transition in such metastable particles. In one case of an Fe−Co alloy precipitate with an especially large free energy driving force (for metal particles) of 0.1 eV/atom, the transformation was shown to occur by homogeneous nucleation at 23 °C in nanocrystal inclusions.[18b]

Essentially all sp^3-hybridized semiconductors undergo a similar four-coordinate to six-coordinate phase transition with increasing pressure, with about a 20% volume contraction. The literature data for each material, as recently reviewed by Ruoff and Li, typically show a rather wide variation of measured upward transition pressure, and wide variability in hysteresis between upward and downward measurements, from experiment to experiment.[19] This variability suggests that extrinsic properties, such as defect concentration and/or deviation from isotropic compression, commonly determine nucleation kinetics. In the previously mentioned GaAs experiments, the hysteresis is larger with solid Ar as a pressure-transmitting medium than with ethanol/methanol.[4] This difference is attributed to reduced shear in solid Ar at high pressure.

MYK predict that bulk Si is kinetically stable up to 64 GPa upon isotropic pressurization. Instability then occurs by the vanishing of the modulus against tetragonal sheer. However, the thermodynamic equilibrium transition pressure is only about 8 GPa, and transition is observed experimentally in the range 8.8−12.5 GPa. MYK suggest that this discrepancy is due to extrinsic nucleation at defects. This in turn suggests that the kinetic barrier might be present in annealed single nanocrystals without defects, such as we model. In the 1950s Turnbull suggested a similar "impurity and/or defect exclusion" hypothesis to explain the very large hysteresis observed in the freezing of fine droplets.[20]

In our coherent model every unit cell simultaneously undergoes a cubic to tetragonal distortion. The activation energy is intracellular and more like that in a molecular isomerization. Some justification for this transition state in small nanocrystals is found in the MYK molecular dynamics simulation. In a system of 216 Si atoms with periodic boundary conditions, simultaneous tetragonal distortion nucleation was observed across the entire sample at 64 GPa. In another molecular dynamics simulation of a diamond phase 54-atom system, a rapid, simultaneous, first-order transition to simple hexagonal phase, with shape change, was observed.[21] Both studies show essentially the type of uniform transition state we model; we additionally include surface energies. With one specific reaction path, the nucleation rate decreases rapidly with increasing size, as the activation energy increases. This contrasts with the classical and defect processes, where the rate increases with increasing size.

B. Metastability in Semiconductor Nanocrystals. In our coherent model, β-tin silicon nanocrystals with bare surfaces become metastable, that is, have half-lives of years or more, very quickly as size increases. Additionally, the classical critical nucleus theory, which should apply to defect-free macroscopic particles, also predicts metastability. *Strain- and defect-free β-tin silicon nanocrystals and microcrystals would appear to be metastable at STP*.

We chose to model the β-tin to diamond transition in silicon as the reaction path was derived by MYK. Actually another transition, β-tin to BC8, is possible and has been observed in pressure release experiments.[22] The BC8 phase shows a distorted, yet crystalline, tetrahedral structure, with a density slightly higher than that of diamond. Substantial activation barriers to this phase should exist as well.

A large piece of β-tin Si would be prone to explosive recrystallization, because 0.25 eV/atom would be liberated upon phase change. In an adiabatic phase change, the diamond product particle would be heated to the melting point. This large heat release and the large activation barrier from the MYK calculation both reflect the strength of the chemical bonding.

The rock salt phase of AlN lies 0.27 eV/atom above wurtzite AlN,[23] essentially as high as β-tin Si above diamond Si. Rock salt AlN is metastable at STP.[1a−c] While we do not know anything about the activation barrier or mechanism in this partially ionic III−V semiconductor, this example shows that very energetic III−V materials can be metastable. Rock salt CdS is also experimentally metastable.[2] In another example, crystalline C_{60} is 0.45 eV/atom above graphite or diamond. Crystalline C_{60} is quite metastable because of the very large change in bonding.

If, as discussed above, nucleation is almost always extrinsic, due to imposed shears and strains or due to extended defects such as dislocations, then it should be possible to stabilize many high-pressure semiconductor phases in nanocrystals. *A wider range of metastable materials may be made as nanocrystals than as bulk crystals*. Nanocrystals are more easily annealed into defect-free structures, because of surface atom mobility. Also, the shape change in a nanocrystal relieves stress that otherwise builds up in macroscopic samples. Recall that stress relief appears to be the cause of the change in kinetics, and the fragmentation into small domains, in the 50 μm GaAs crystals with pressure cycling.

Finally, we suggest that manipulation of surface energy provides a way to additionally stabilize the high-pressure phase in nanoparticles. Thermal annealing at high pressure should create create a minimal energy (round in our model), more stable shape, before pressure release. Also, chemical passivation at high pressure may lower the surface energy of the high-pressure phase and provide additional kinetic stability. Also, the quite remarkable example of rock salt cadmium sulfide[2] shows that it is possible, at least in this one case, to kinetically induce the nucleation and growth of high-pressure phases at STP.

Acknowledgment. We thank A. P. Alivisatos and S. Tolbert for extensive discussion and correspondence on this subject. We also thank J. C. Tully, K. Raghavachari, and D. W. Murphy for their advice concerning a preliminary version of this manuscript.

JA954166P

(17) Oslon, G.; Cohen, M. In *Dislocations in Solids*; Narbarro, F., Ed.; North-Holland: Amsterdam, 1986; Vol. 7, Chapter 7.

(18) (a) Easterling, K.; Swann, P. *Acta Metall.* **1971**, *19*, 117. (b) Lin, M.; Olson, G.; Cohen, M. *Acta Metall. Mater.* **1993**, *41*, 253.

(19) Ruoff, A.; Li, T. *Annu. Rev. Mater. Sci.* **1995**, *25*, 249.

(20) (a) Turnbull, D. *J. Chem. Phys.* **1952**, *20*, 411. (b) Turnbull, D. *J. Appl. Phys* **1950**, *21*, 1022.

(21) Focher, P.; et al. *Europhys. Lett.* **1994**, *26*, 345.

(22) (a) Crain, J.; et al. *Phys. Rev.* **1994**, *B49*, 5327. (b) Biswas, R.; Martin, R.; Needs, R.; Nelson, O. *Phys. Rev.* **1984**, *B30*, 3210.

(23) Christensen, N.; Gorczyca, I. *Phys. Rev.* **1993**, *B47*, 4307.